



ATLAS jet and missing-ET reconstruction, calibration, and performance

Peter Berta

On behalf of the ATLAS Collaboration

Faculty of Mathematics and Physics, Charles University in Prague, V Holesovickach 2, Prague 8, Czech Republic

Abstract

The ATLAS experiment has achieved a very high precision on jet and missing transverse energy performance by the use of advanced calorimeter-based topological clustering and local cluster calibration, event-by-event pile-up subtraction methods, and in situ techniques to correct for the residual jet energy response difference between data and simulation. Tracking information is being combined with calorimeter to further improve the jet and missing transverse energy performance. ATLAS has also commissioned several new powerful tools for the analysis and interpretation of hadronic final states at the LHC such as jet substructure, jet mass, quark-gluon discrimination, and jet tagging tools for the identification of boosted heavy particles. An overview of the reconstruction, calibration, and performance of jets, missing transverse energy, jet substructure, and jet tagging at ATLAS is presented.

Keywords: LHC, ATLAS, jets, missing transverse energy, jet substructure

1. Introduction

Jets and missing transverse energy (E_T^{miss}) are key ingredients of many Standard Model measurements and New Physics searches at the ATLAS experiment [1]. Large data samples were recorded during the LHC running in years 2010–2012. Complex clustering and calibration algorithms for the reconstruction of jets, E_T^{miss} , and jet substructure have been developed and commissioned. These algorithms can challenge the difficulties connected with high luminosity environment at the LHC.

2. Jet reconstruction, calibration and performance

One of the challenges connected with jet reconstruction are simultaneous proton-proton collisions in the same or neighboring bunch crossings (pile-up). The effect of pile-up is twofold: it adds energy deposits to the jets from the hard-scatter event and it creates additional jets (pile-up jets).

The highly segmented calorimeters of the ATLAS detector enable to reconstruct jets with high precision. The calorimeter cells are grouped to 3-dimensional clusters of topologically connected cells called topo-clusters. Then, jets can be built from topo-clusters using arbitrary clustering algorithm. The resulting jets are corrected for the effect of pile-up. The direction of the jet is adjusted in the jet origin correction. This is followed by the jet calibration derived using Monte Carlo (MC) simulations and residual in situ calibration applied to jets in data only. The pile-up jets can be filtered using information from tracks. The following sections provide more details about all these steps.

2.1. Topo-clusters

The topo-cluster finding is optimized to noise and pile-up suppression [2]. The first step is the identification of seeds which are cells with energy deposits $E > 4\sigma$ where σ is the noise defined as a sum in quadrature of electronic and pile-up noise. The second step is the iterative adjunction of neighboring cells with $E > 2\sigma$ to the seeds. In the third step, an extra layer of

Email address: peter.bertha@cern.ch ()



cells with $E > 0$ on the perimeter of the clustered cells are added. Splitting algorithm separates the resulting topo-clusters based on local energy maxima.

There are two options to calibrate topo-clusters: calibration to the electromagnetic scale (EM topo-clusters) and local calibration weighting [3] (LCW topo-clusters). In both cases, the mass of the topo-clusters is set to zero. The EM topo-clusters are calibrated to the response from electrons while the LCW topo-clusters are classified as electromagnetic or hadronic and then a weighting scheme corrects for the different electron-to-pion response in the calorimeters. Dead material correction and out-of-cluster correction is used for the LCW topo-clusters.

2.2. Jet finding

The standard jet finding algorithm at ATLAS experiment is the anti- k_r clustering algorithm [4] with distance parameters $R = 0.4$ and $R = 0.6$. The input to the jet finding algorithm are EM and LCW topo-clusters resulting in EM and LCW jets, respectively. Additionally, clustering algorithms with large distance parameters (large- R) have been commissioned and are used, such as anti- k_r algorithm with $R = 1.0$ and Cambridge-Aachen (C/A) algorithm [5] with $R = 1.2$.

2.3. Pile-up correction

The topo-cluster finding suppresses the effect of pile-up but applying a further pile-up correction on the jets is necessary. For 2011 data, the offset correction [6] was used to correct the jet transverse momentum, p_T , by an offset. This offset was determined from MC simulations as a function of the number of primary vertices, N_{PV} , and the instantaneous luminosity in the given event. For 2012 data, jet-area-based correction [7] was used followed by residual offset correction [8]. The jet-area-based correction corrects the jet p_T event-by-event and jet-by-jet based on the relation:

$$p_T^{\text{corr}} = p_T - A \cdot \rho \quad (1)$$

where A is the jet area and ρ is the pile-up p_T density in the event. The Figure 1 shows the performance of the pile-up correction for 2012 MC simulation. The jet-area-based correction highly reduces the jet p_T dependence on the pile-up which is entirely removed after residual offset correction for all jet pseudorapidities.

2.4. Jet origin correction

The jet origin correction [9] makes the jet pointing back to the primary event vertex instead of the nominal center of the ATLAS detector.

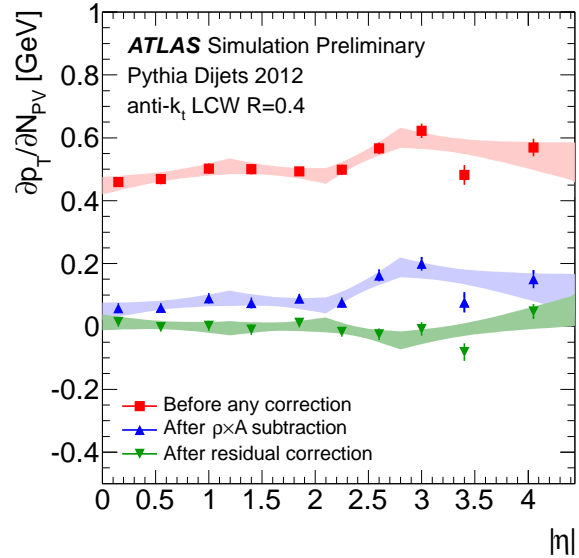


Figure 1: The slope of the jet p_T dependence on N_{PV} as a function of jet pseudorapidity before any correction, after jet-area-based correction, and after residual offset correction in simulated dijets events, [8].

2.5. Jet calibration

The jet energy and pseudorapidity are calibrated using the relation between reconstructed and truth-jets in MC simulated QCD events [9]. The jet energy calibration (Jet Energy Scale) is a multiplication by the inverse of average jet energy response. The Figure 2 shows the dependence of the jet energy response on pseudorapidity. After applying the jet energy scale (JES), the EM jets and LCW jets are called EM+JES and LCW+JES jets, respectively. The jet pseudorapidity calibration corrects for a bias due to poorly instrumented regions of the calorimeter. Average difference between pseudorapidities of reconstructed and truth-jets in MC is added as a correction factor to the jet pseudorapidity.

Differences between data and MC simulation lead to miscalibration of jet energy which is removed by a residual in situ calibration applied to the data only. It corrects the jet p_T by multiplying by the response ratio of MC to data

$$\frac{\text{Response}_{\text{MC}}}{\text{Response}_{\text{Data}}} = \frac{\langle p_T^{\text{jet}} / p_T^{\text{ref}} \rangle_{\text{MC}}}{\langle p_T^{\text{jet}} / p_T^{\text{ref}} \rangle_{\text{Data}}}, \quad (2)$$

where the response is obtained from transverse momentum balance between jet and a reference object. To cover large kinematic phase space, different reference objects are used in the following methods: dijets η -

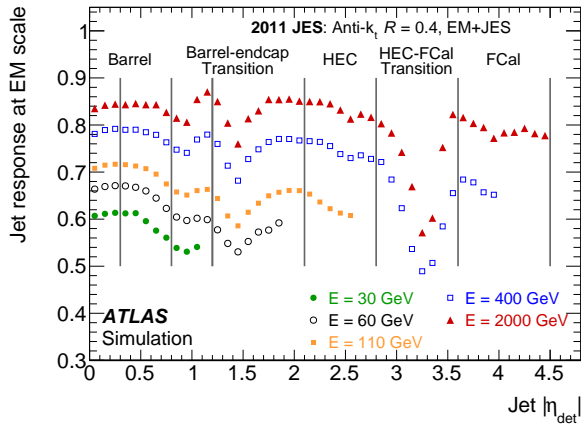


Figure 2: Average response of simulated EM jets as a function of jet pseudorapidity for several truth-jet energies. Also indicated are the different calorimeter regions, [9].

intercalibration, γ +jet balance, Z+jet balance and multi-jet balance.

The uncertainty of JES has several components, such as in situ calibration uncertainties, pile-up uncertainty, flavor composition and flavor response uncertainty. These uncertainties for the central region are shown in Figure 3 together with the total JES uncertainty. The JES uncertainty is generally smaller than 4% and in the jet p_T region of 100 – 1000 GeV, it is less than 2%.

2.6. Jet Energy Resolution

The jet energy resolution is measured in data with two in situ techniques: dijet balance and bisector method, [11]. The Figure 4 shows the jet energy resolution obtained with bisector method for both type of calibration of jets. The LCW+JES jets exhibit better energy resolution than EM+JES jets.

2.7. Suppression of pile-up jets

To suppress pile-up jets against hard-scatter jets, information from tracks matched to each jet is used which is implemented in several methods [13]. One commonly used approach evaluates a discriminating variable for each jet called Jet Vertex Fractions (JVF) which is defined as the fraction of momenta of tracks matched to the jet which are associated with the hard-scatter vertex. Larger discriminating power can be achieved with the variable Jet Vertex Tagger (JVT) which uses multivariate combination of two track-based variables. The Figure 5 shows the pile-up dependence of efficiency for

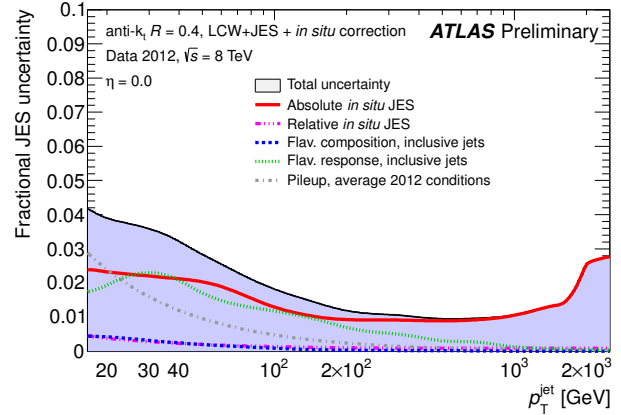


Figure 3: Fractional jet energy scale systematic uncertainty components as a function of p_T for anti- k_t jets with radius parameter of $R = 0.4$ at $|\eta| = 0$ calibrated using the LCW+JES calibration scheme. The total uncertainty (all components summed in quadrature) is shown as a filled blue region topped by a solid black line. Average 2012 pileup conditions were used, and topology dependent components were taken from inclusive dijet samples, [10].

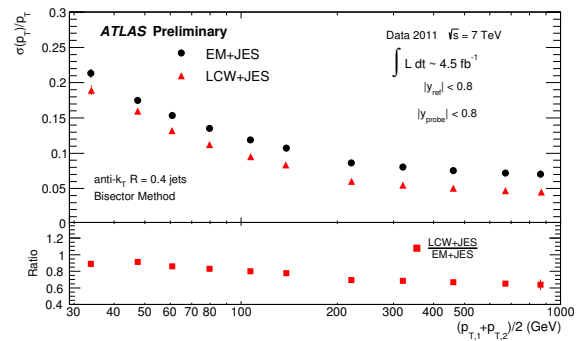


Figure 4: Fractional jet energy resolution for anti- k_t $R = 0.4$ jets as a function of the average jet transverse momenta measured with the bisector in-situ technique using the EM+JES calibration (circles) and the LCW+JES calibration (triangles) with 2011 data. The bottom plot shows the ratio as a function of the average jet transverse momenta, [12].

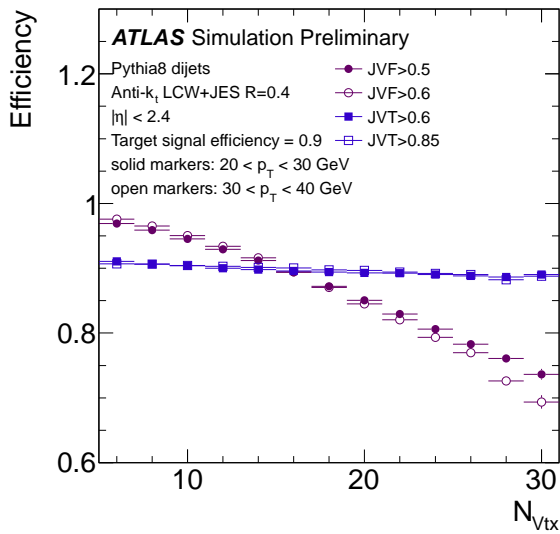


Figure 5: N_{pV} dependence of the hard-scatter jet efficiency for fixed cuts of JVT (blue) and JVF (violet) chosen such that the inclusive efficiency is 90%. The cut values imposed on JVT and JVF, which depend on the p_T bin, are specified in the legend, [13].

fixed cuts of JVT and JVF for hard-scatter jets. The efficiency of selection using JVT has smaller pile-up dependence than the efficiency of selection using JVF.

3. Jet Substructure

Jets are commonly used as a stand-in for 4-momenta of generic partons. Except this basic usage, the jet components may be exploited in several jet substructure techniques [14]. They are used for identification of boosted hadronically decaying objects and discrimination between quark- and gluon-initiated jets.

3.1. Boosted hadronically decaying objects

Boosted hadronically decaying objects, such as top quarks, W , Z , and Higgs bosons, can be identified at the ATLAS experiment using jet substructure techniques [15]. Generally, the topo-clusters are clustered to large- R jets, and then the internal structure of large- R jets can discriminate between signal (boosted objects) and background jets. To remove the effect of pile-up in large- R jets, selective removal of soft radiation (grooming) may be applied. Several grooming techniques such as filtering [16], trimming [17], and pruning [18] can be used. The Figure 6 shows the jet mass distribution before and after trimming for signal jets (hadronically decaying Z boson) and background jets (dijet events). One can see

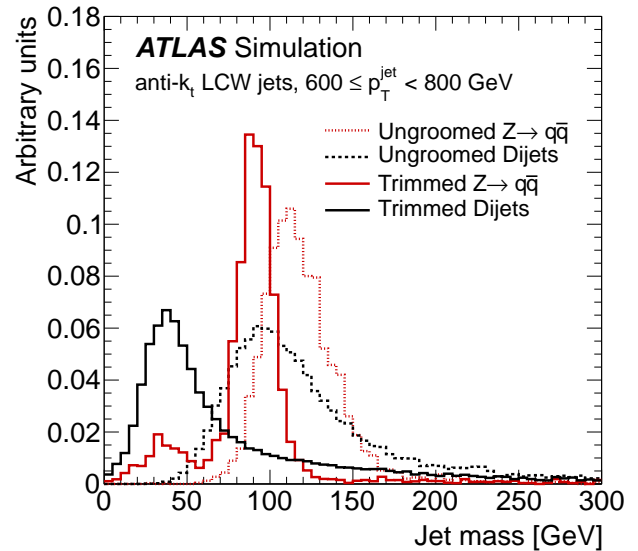


Figure 6: Leading- p_T jet mass distribution for simulated hadronically decaying Z boson signal events (red) compared to dijet background events. The dotted lines show the ungroomed jet distributions, whereas the solid lines show the trimmed jet distributions, [15].

that the trimming pushes the jet mass peak for signal jets back to the Z boson mass, and the discrimination power between signal and background jets is improved after the trimming.

Several substructure techniques for identification of boosted hadronically decaying objects were commissioned at the ATLAS experiment such as shower deconstruction [19], Q-jets [20], HEPTopTagger [21], and tagging with jet shapes [22]. The summary of the achieved performance for boosted top quark identification is plotted in Figure 7. The tagging using jet shapes has the best performance for higher signal efficiencies while the shower deconstruction technique has the best performance when higher background rejection is required.

3.2. Quark-gluon discrimination

The discrimination between quark- and gluon-initiated jets may be useful for identification of hadronic decays of W and Z bosons. A likelihood based discriminant using two variables constructed from associated tracks can be used to enhance the abundance of quark-initiated jets [23]. Figure 8 shows the performance of such discriminant for jets in data and MC simulation with Pythia 6 [24] and Herwig++ [25] generators. Disagreement between data and MC simulation is observed. In data, quark- and gluon-initiated jets look

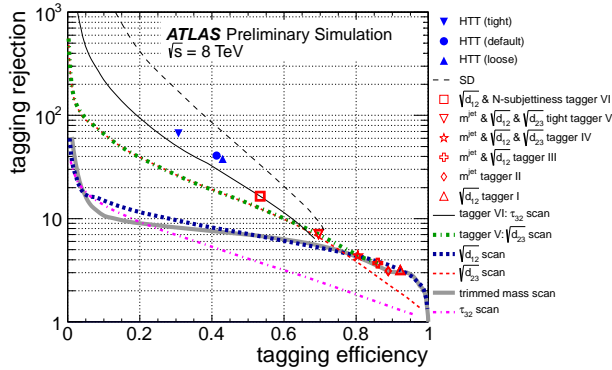


Figure 7: The dependence of the light-jet rejection rate on the top-jet tagging efficiency for different taggers. All substructure taggers and scans use trimmed anti- k_r $R = 1.0$ jets. The HEPTopTagger (points labelled HTT) uses C/A $R = 1.2$ jets that are geometrically matched to the anti- k_r jets, [21].

more similar to each other than in the Pythia 6 simulation and less similar than in the Herwig++ simulation.

4. Missing Transverse Energy

The E_T^{miss} is an important signature for many physics processes. It is an event quantity calculated based on momentum conservation in the transverse plane [26]:

$$E_T^{\text{miss}} = \sqrt{(E_x^{\text{miss}})^2 + (E_y^{\text{miss}})^2},$$

$$E_{x(y)}^{\text{miss}} = -\left(E_{x(y)}^{\text{jets}} + E_{x(y)}^e + E_{x(y)}^\gamma + E_{x(y)}^\tau + E_{x(y)}^\mu + E_{x(y)}^{\text{ST}}\right) \quad (3)$$

where $E_{x(y)}^{\text{jets}}$, $E_{x(y)}^e$, $E_{x(y)}^\gamma$, $E_{x(y)}^\tau$, and $E_{x(y)}^\mu$ are the sum of $x(y)$ -component of the momenta of all jets, electrons, photons, taus and muons in the event, respectively. All objects are corrected for the pile-up and calibrated. The anti- k_r $R = 0.4$ jets calibrated with LCW+JES scheme with $p_T > 20$ GeV are used to calculate $E_{x(y)}^{\text{jets}}$. Suppression of pile-up jets is done by rejecting jets with $\text{JVF} = 0$, $p_T < 50$ GeV and $|\eta| < 2.4$. The E_T^{miss} Soft Term, $E_{x(y)}^{\text{ST}}$, is defined as the sum of $x(y)$ -component of the momenta of all topo-clusters and tracks not associated to the above physics objects with double counting avoided.

The pile-up has large effect on the performance of E_T^{miss} reconstruction. There are several pile-up correction methods for E_T^{miss} , [27]. All methods corrects the E_T^{miss} Soft Term. The first method called Soft-Term Vertex-Fraction (STVF) corrects the E_T^{miss} Soft Term by a multiplication factor constructed from all tracks in the event. This factor is the fraction of momenta of tracks

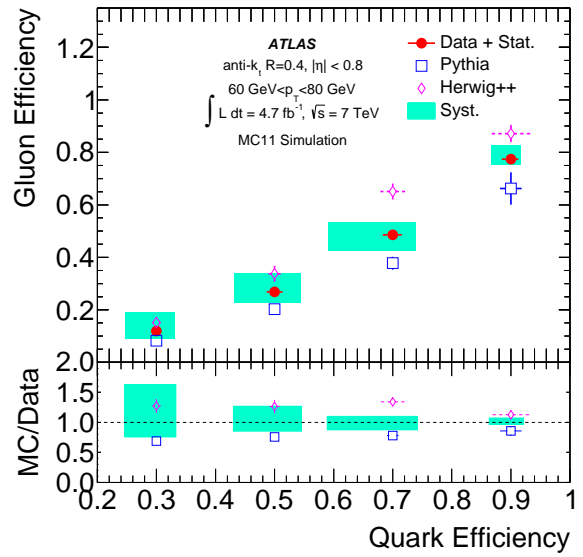


Figure 8: Gluon-jet efficiency as a function of quark-jet efficiency calculated using jet properties extracted from data (solid symbols) and from MC simulated jets from the dijet Pythia 6 (empty squares) and Herwig++ (empty diamonds) samples. The shaded band shows the total systematic uncertainty on the data. The bottom panel shows the ratios of each MC simulation to the data. The error bands on the performance in the data are drawn around 1.0, [23].

matched to the hard-scatter vertex. Further possibilities are to use jet-area-based methods. The basic idea in these methods is that the soft term constituents are clustered to jets which are corrected with jet-area-based pile-up correction method. Optionally, JVF based selection can be applied. The Figure 9 shows the pile-up dependence of reconstructed average E_T^{miss} for several pile-up correction methods. The E_T^{miss} corrected with STVF method gives the smallest bias.

5. Conclusions

The ATLAS experiment has developed and commissioned several techniques to reconstruct jets and mitigate pile-up effects on jets and E_T^{miss} . High precision has been obtained for the JES in 2012 with the in situ techniques. Methods based on tracks have been used to filter pile-up jets and to scale the E_T^{miss} Soft Term. Moreover, jet substructure is exploited as a powerful tool for identifying boosted hadronically decaying objects.

References

- [1] ATLAS Collaboration, The ATLAS Experiment at the CERN Large Hadron Collider, JINST 3 (2008) S08003. doi:10.1088/1748-0221/3/08/S08003.

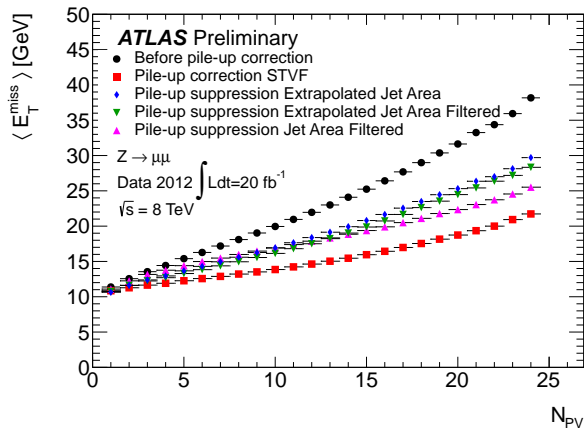


Figure 9: The reconstructed average E_T^{miss} as a function of N_{pV} for the inclusive $Z \rightarrow \mu\mu$ data sample for several pile-up correction methods, [27].

- [2] W. Lampl, et al., Calorimeter clustering algorithms: description and performance (ATL-LARG-PUB-2008-002). URL <http://cdsweb.cern.ch/record/1099735>
- [3] T. Barillari, et al., Local hadronic calibration (ATL-LARG-PUB-2009-001). URL <http://cdsweb.cern.ch/record/1112035>
- [4] M. Cacciari, G. P. Salam, G. Soyez, The anti- k_r jet clustering algorithm, JHEP 04 (2008) 063. arXiv:0802.1189, doi:10.1088/1126-6708/2008/04/063.
- [5] Y. L. Dokshitzer, G. Leder, S. Moretti, B. Webber, Better jet clustering algorithms, JHEP 08 (1997) 001. arXiv:hep-ph/9707323, doi:10.1088/1126-6708/1997/08/001.
- [6] ATLAS Collaboration, Pile-up corrections for jets from proton-proton collisions at $\sqrt{s} = 7$ TeV in ATLAS in 2011 (ATLAS-CONF-2012-064). URL <http://cdsweb.cern.ch/record/1459529>
- [7] M. Cacciari, G. P. Salam, Pileup subtraction using jet areas, Phys. Lett. B 659 (2008) 119. arXiv:0707.1378, doi:10.1016/j.physletb.2007.09.077.
- [8] ATLAS Collaboration, Pile-up subtraction and suppression for jets in ATLAS (ATLAS-CONF-2013-083). URL <http://cdsweb.cern.ch/record/1570994>
- [9] ATLAS Collaboration, Jet energy measurement and its systematic uncertainty in proton-proton collisions at $\sqrt{s} = 7$ TeV with the ATLAS detector (CERN-PH-EP-2013-222). arXiv:1406.0076.
- [10] Atlas public results. URL <https://twiki.cern.ch/twiki/bin/view/AtlasPublic/JetEtmisApproved2013JESUncertainty>
- [11] ATLAS Collaboration, Jet energy resolution in proton-proton collisions at $\sqrt{s} = 7$ TeV recorded in 2010 with the ATLAS detector, Eur. Phys. J. C 73 (2013) 2306. arXiv:1210.6210, doi:10.1140/epjc/s10052-013-2306-0.
- [12] Atlas public results. URL <https://twiki.cern.ch/twiki/bin/view/AtlasPublic/JetEtmisApproved2013Jer2011>
- [13] ATLAS Collaboration, Tagging and suppression of pileup jets with the ATLAS detector (ATLAS-CONF-2014-018). URL <http://cdsweb.cern.ch/record/1700870>
- [14] A. Altheimer, et al., Jet Substructure at the Tevatron and LHC: New results, new tools, new benchmarks, J. Phys.

G 39 (2012) 063001. arXiv:1201.0008, doi:10.1088/0954-3899/39/6/063001.

- [15] ATLAS Collaboration, Performance of jet substructure techniques for large- R jets in proton-proton collisions at $\sqrt{s} = 7$ TeV using the ATLAS detector, JHEP 09 (2013) 076. arXiv:1306.4945.
- [16] J. M. Butterworth, et al., Jet substructure as a new Higgs search channel at the LHC, Phys. Rev. Lett. 100 (2008) 242001. arXiv:0802.2470, doi:10.1103/PhysRevLett.100.242001.
- [17] D. Krohn, J. Thaler, L.-T. Wang, Jet Trimming, JHEP 02 (2010) 084. arXiv:0912.1342, doi:10.1007/JHEP02(2010)084.
- [18] S. D. Ellis, C. K. Vermilion, J. R. Walsh, Recombination Algorithms and Jet Substructure: Pruning as a Tool for Heavy Particle Searches, Phys. Rev. D 81 (2010) 094023. arXiv:0912.0033, doi:10.1103/PhysRevD.81.094023.
- [19] ATLAS Collaboration, Performance of shower deconstruction in ATLAS (ATLAS-CONF-2014-003). URL <http://cdsweb.cern.ch/record/1648661>
- [20] ATLAS Collaboration, Performance and Validation of Q-Jets at the ATLAS Detector in pp Collisions at $\sqrt{s}=8$ TeV in 2012 (ATLAS-CONF-2013-087). URL <http://cdsweb.cern.ch/record/1572981>
- [21] ATLAS Collaboration, Performance of boosted top quark identification in 2012 ATLAS data (ATLAS-CONF-2013-084). URL <http://cdsweb.cern.ch/record/1571040>
- [22] ATLAS Collaboration, Performance of Boosted W Boson Identification with the ATLAS Detector (ATL-PHYS-PUB-2014-004). URL <http://cdsweb.cern.ch/record/1690048>
- [23] ATLAS Collaboration, Light-quark and gluon jet discrimination in pp collisions at $\sqrt{s}=7$ TeV with the ATLAS detector, Eur. Phys. J. C 74 (2014) 3023. arXiv:1405.6583, doi:10.1140/epjc/s10052-014-3023-z.
- [24] T. Sjostrand, S. Mrenna, P. Z. Skands, PYTHIA 6.4 Physics and Manual, JHEP 0605 (2006) 026. arXiv:hep-ph/0603175, doi:10.1088/1126-6708/2006/05/026.
- [25] M. Bahr, et al., Herwig++ physics and manual, Eur. Phys. J. C 58 (2008) 639. arXiv:0803.0883, doi:10.1140/epjc/s10052-008-0798-9.
- [26] ATLAS Collaboration, Performance of Missing Transverse Momentum Reconstruction in ATLAS studied in Proton-Proton Collisions recorded in 2012 at 8 TeV (ATLAS-CONF-2013-082). URL <http://cdsweb.cern.ch/record/1570993>
- [27] ATLAS Collaboration, Pile-up Suppression in Missing Transverse Momentum Reconstruction in the ATLAS Experiment in Proton-Proton Collisions at $\sqrt{s} = 8$ TeV (ATLAS-CONF-2014-019). URL <http://cdsweb.cern.ch/record/1702055>